Electronic Supplementary Material for

Controlling magnetic coupling in bi-magnetic nanocomposites

F. Sayed[1], *G. Muscas*[2], *S. Jovanovic*[3,4], *G. Barucca*[5], *F. Locardi*[6], *G. Varvaro*[7], *D. Peddis*[6,7], *R. Mathieu*[1], *T. Sarkar*[1*]

[1]Department of Engineering Sciences, Uppsala University, Box 534, SE-75121 Uppsala, Sweden

[2]Department of Physics and Astronomy, Uppsala University, Box 516, SE-75120 Uppsala, Sweden

[3]Advanced Materials Department, Jožef Stefan Institute, 1000 Ljubljana, Slovenia

[4]Laboratory of Physics, Vinča Institute of Nuclear Sciences, University of Belgrade, 11000 Belgrade, Serbia

[5]Department SIMAU, University Politecnica delle Marche, Via Brecce Bianche, Ancona, 60131, Italy

[6]Dipartimento di Chimica e Chimica Industriale, Università degli Studi di Genova, Via Dodecaneso 31, Genova, 16146, Italy

[7]Istituto di Struttura della Materia – CNR, Area della Ricerca di Roma1, Monterotondo Scalo, RM, 00015, Italy

[*]**Corresponding author:** tapati.sarkar@angstrom.uu.se

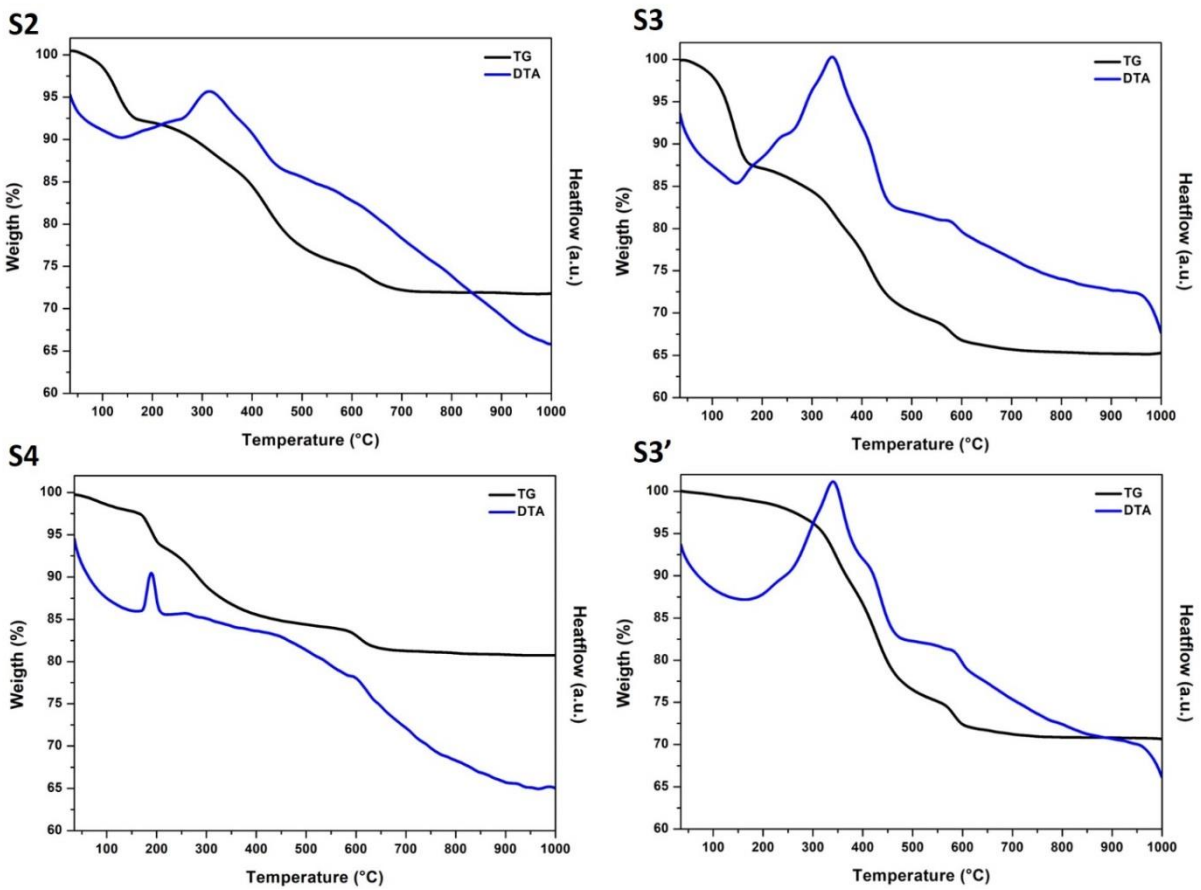

Fig. S1. DTA/TG curves of S2, S3, S4, and S3′.

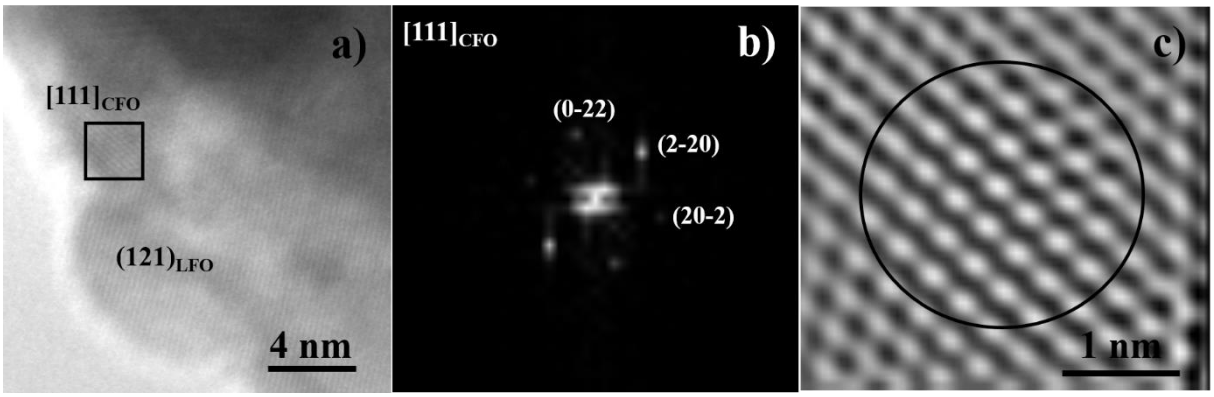

Fig. S2. S4′ sample: a) HR-TEM image, b) Fast Fourier Transform (FFT) of the area indicated by a square in a) revealing the presence of a small CFO nanocrystal in [111] zone axis, and c) image of the area indicated by a square in a) where the noise was removed.

Fig. S2 c) was obtained by removing the noise from the part of the image evidenced by a square in S2 a) by using the Gatan Microscopy Suite GMS3 software [http://www.gatan.com/products/tem-analysis/gatan-microscopy-suite-software].

The typical approach consists of the FFT of the image, the application of a mask to remove the noise and an inverse FFT to reobtain the image. The hexagonal symmetry of the [111] CFO crystal is clearly evidenced in this way, and it is possible to observe that it is only about 2 nm in size.

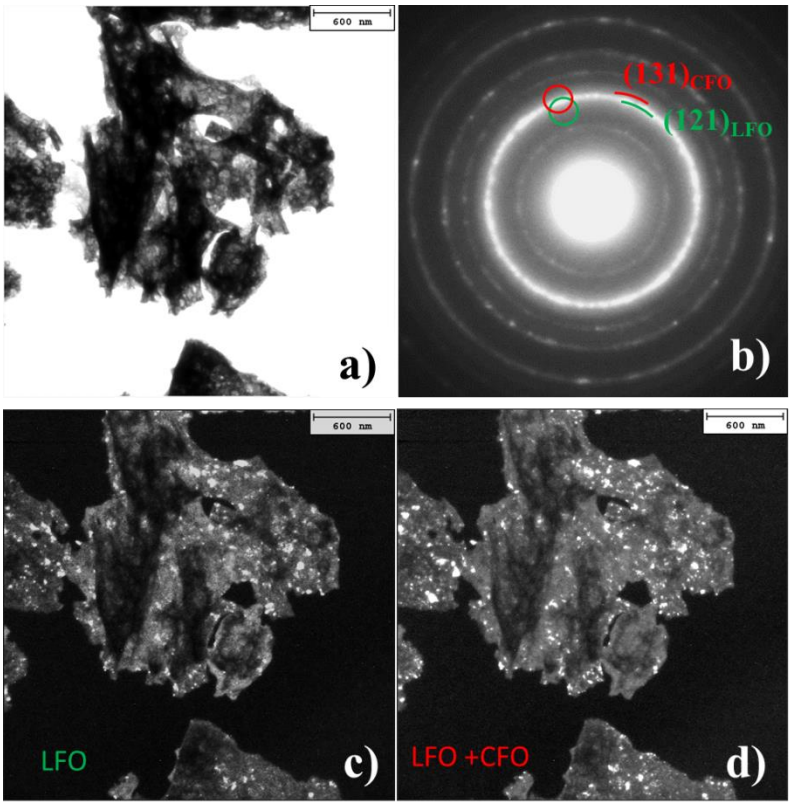

Fig. S3. Sample S4′: (a) TEM bright field image, (b) corresponding selected area electron diffraction pattern taken on a large area of the sample, (c) dark field image highlighting the presence and distribution of LFO nanocrystals, and (d) dark field image highlighting the presence and distribution of LFO and CFO nanocrystals.

The small dimension of the CFO nanocrystals and their distribution were further investigated in the S4′ sample by TEM dark field analysis performed on large areas of the sample. Fig. S3b shows the SAED pattern taken on a large region of the sample imaged in Fig. S3a. The intensity of the CFO diffraction ring is low and diffuse compared with the LFO ones, thus revealing a lower size of the CFO crystals compared to the LFO ones. The image in Fig. S3c was obtained using a portion of the most intense LFO diffraction ring (corresponding to the {121} lattice planes) indicated by the green circle in Fig. S3b. Thus, the visible crystals in the image are LFO nanocrystals. Next, the selected area was moved in the red circle position and the most intense CFO diffraction ring was taken (corresponding to the {131} lattice planes). In Fig. S3d, both the previous LFO and the new CFO crystals are lighted. Comparing the two images, it is very difficult to observe big differences, and this reveals that the CFO crystals are very small (hence hardly visible at this magnification) and probably they are also well dispersed in the sample because, otherwise, large areas of the sample, where CFO crystals were aggregated, could appear lighted.

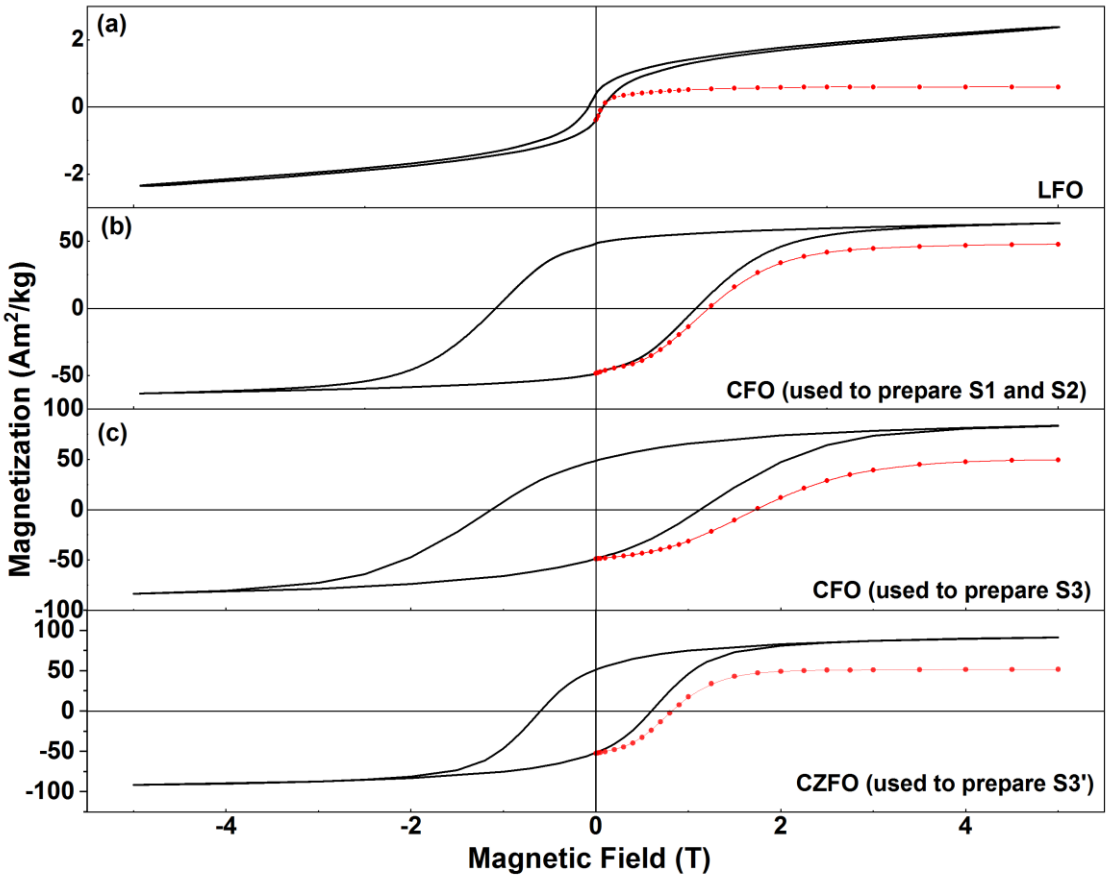

Fig. S4. Isothermal field-dependent magnetization (black lines) and M_{DCD} versus reverse magnetic field (red symbols) of the pure phases (LFO, CFO, and CZFO) recorded at T = 5 K.

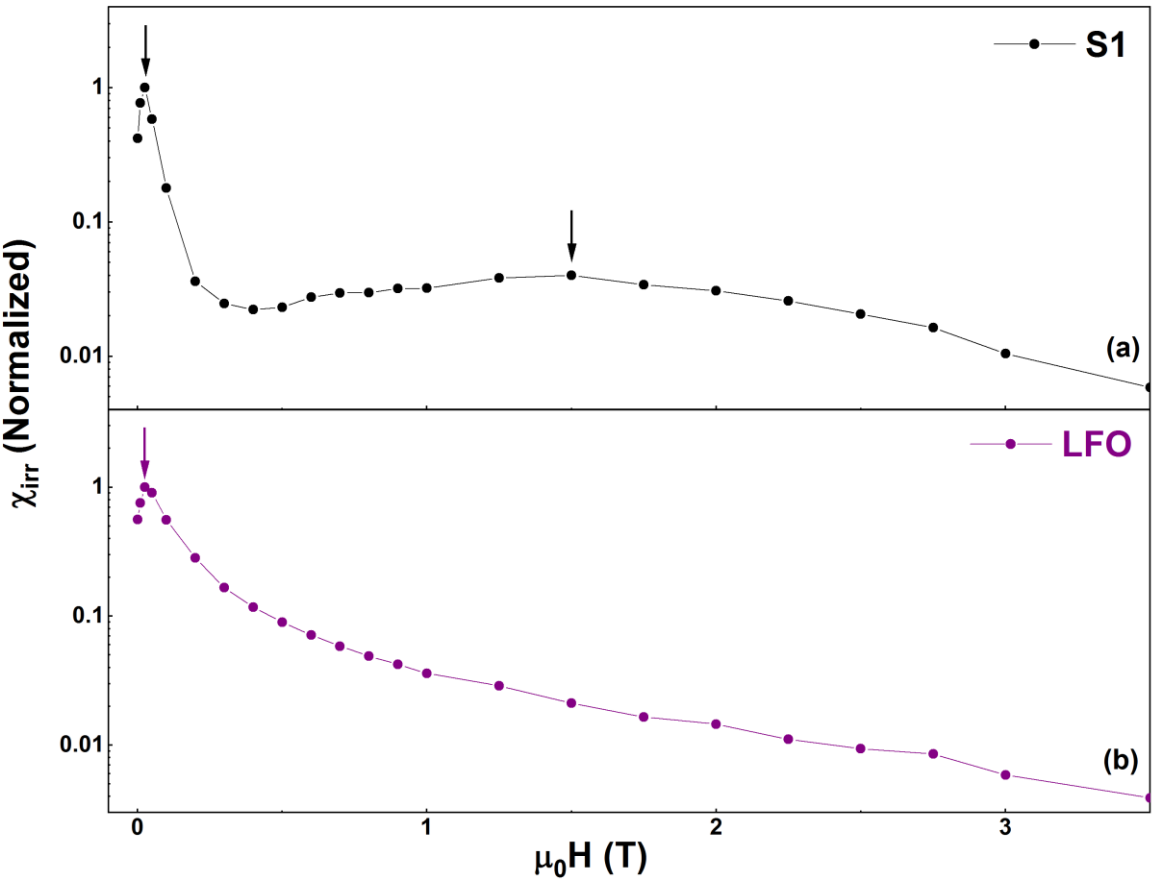

Fig. S5. Switching field distributions of (a) S1 and (b) LFO as obtained from the first order derivatives of the corresponding M_{DCD} curves.

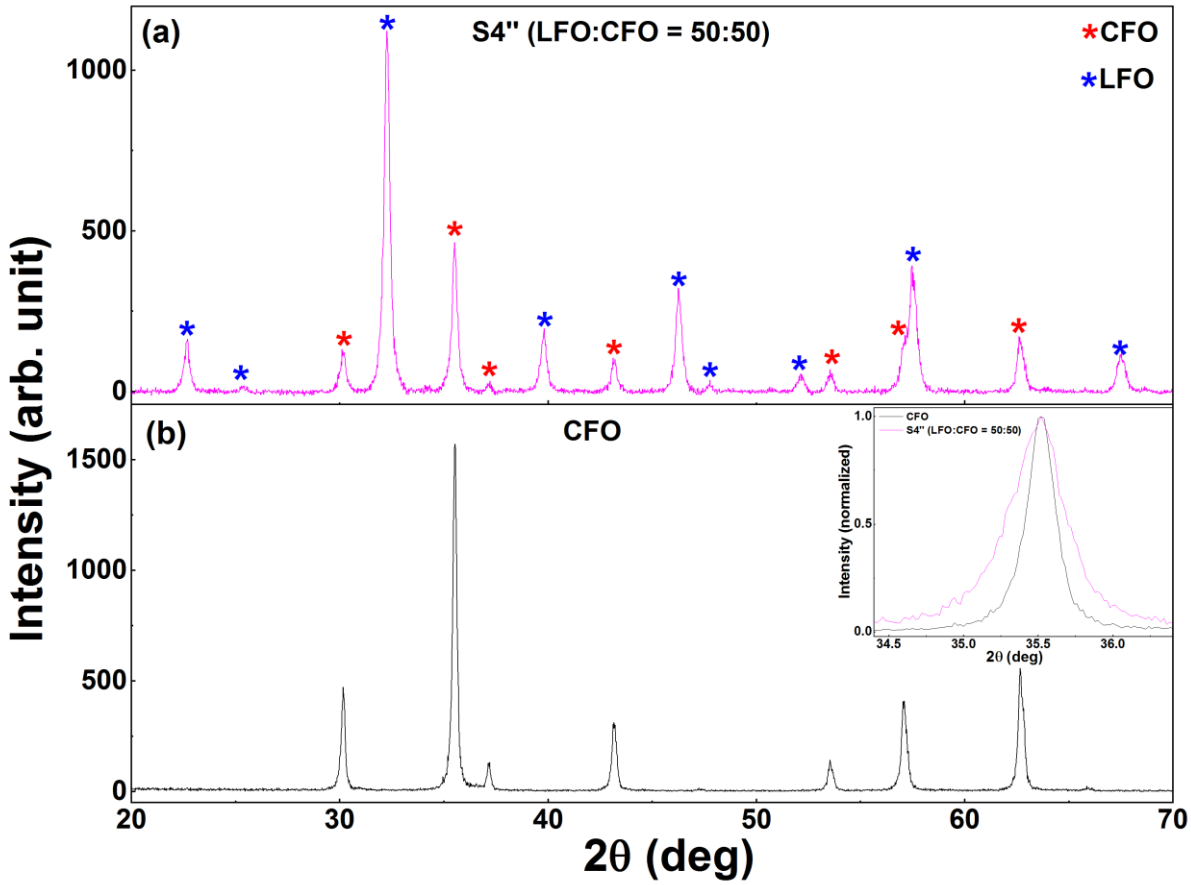

Fig. S6. XRPD patterns of (a) S4′′ and (b) CFO. The reflections corresponding to CFO and LFO in (a) are shown by red and blue asterisks, respectively. The inset in (b) shows the enlarged region around the strongest reflection corresponding to CFO. The data in the inset has been normalized with respect to the maximum intensity value of the strongest reflection of CFO, for easy comparison of the respective peak widths.